Global scaling behaviors and chaotic measure characterized by the convergent rates of period-p-tupling bifurcations

Shou-Li Peng[1,2,3] and Ke-Fei Cao[2,1,*]
[1]*Laboratory of Nonlinear Complex Systems, Department of Physics and Institute of Applied Mathematics of Yunnan Province, Yunnan University, Kunming, Yunnan 650091, China*
[2]*China Center of Advanced Science and Technology (World Laboratory), P.O. Box 8730, Beijing 100080, China*
[3]*Yunnan Observatory, Chinese Academy of Sciences, P.O. Box 110, Kunming, Yunnan 650011, China*
(Received 17 July 1995; revised manuscript received 22 March 1996)

The Derrida-Gervois-Pomeau composition of the sequences $\mathbf{Q}*$ is a topological conjugate compression operation. On the basis of the numerical calculation for the quadratic map $f_\lambda(x)=1-\lambda x^2$, it is found that $\mathbf{Q}*$ has the uniform compression ratio $\delta^{-1}(\mathbf{Q})$, i.e., the reciprocal of the universal convergent rate. A series of global scaling behaviors relating to the periodic windows, the window bands, and the steps of equal topological entropy class (ETEC) are revealed to be independent of the sequences. In particular, the geometric interpretation for the Yorke-Grebogi-Ott-Tedeschini-Lalli normalized crisis value of ''windows'' $\mu_c=\frac{9}{4}$ is given clearly through the scaling for the ETEC steps. The universal positions of superstable points in all the periodic windows are determined by the window scaling ratios $\gamma_{\rm PDB}=1$ for the period-doubling bifurcation (PDB) sequences and $\gamma_N=\frac{1}{3}$ for the non-PDB sequences. The approximate analytic formula of the chaotic measure is obtained by employing the convergent rates δ of periodic sequences. The singularity spectrum and the generalized fractal dimension of the chaotic set are also calculated. These results imply that the metric universality of the periodic sequences may be a very good complete description for the topological space of two symbols. [S1063-651X(96)05609-7]

PACS number(s): 05.45.+b, 03.20.+i, 05.20.Gg, 05.70.Jk

I. INTRODUCTION

The discovery of metric universalities is a milestone of nonlinear science [1]. These metric universalities originate from the generalized Feigenbaum renormalization-group equation and its eigenvalues δ. Recently, we found the devil's staircase of topological entropy in the interval dynamics [2–4], which has cleared the concept of topological equivalence class, i.e., the step of equal topological entropy class (ETEC) generated by the topological conjugate operation $\mathbf{Q}*$ of Derrida, Gervois, and Pomeau [5,6] [see Sec. II A for the definition of the Derrida-Gervois-Pomeau (DGP) $*$ composition rule]. On the basis of this, we further reveal in this paper some global and fine regularities and deepen the understanding of the universal constant δ: $\delta(\mathbf{Q})$ reflects not only the convergent rate for the period-p-tupling bifurcation $\mathbf{Q}*^n$ (p is the period of sequence $\mathbf{Q}$) but also, more important, the compression ratio of the topological conjugate operation $\mathbf{Q}*$. In general, we can define the compression ratio $\eta(\mathbf{Q})$ of the topological conjugate operation $\mathbf{Q}*$ as

$$|\mathbf{Q}*[\mathbf{W}_1,\mathbf{W}_2]|=\eta(\mathbf{Q})|[\mathbf{W}_1,\mathbf{W}_2]|, \qquad (1.1)$$

where $\mathbf{Q}*[\mathbf{W}_1,\ \mathbf{W}_2]\equiv[\mathbf{Q}*\mathbf{W}_1,\ \mathbf{Q}*\mathbf{W}_2]$ and $|\,|$ is the parametric metric or norm for the set of words (sequences) [2–4], i.e., $|[\mathbf{W}_1,\ \mathbf{W}_2]|\equiv\lambda(\mathbf{W}_2)-\lambda(\mathbf{W}_1)$, with $\lambda(\mathbf{W}_1)$ and $\lambda(\mathbf{W}_2)$ two parameter values corresponding to the characteristic words that denote the boundaries (the minimal $\mathbf{W}_1$ and the maximal $\mathbf{W}_2$) of the set of words considered. It is known that the parameter values $\lambda(\mathbf{W})$ and $\lambda(\mathbf{Q}*\mathbf{W})$ can be calculated by the Kaplan algorithm [7], which is the standard method of applying the operation of contracting fixed point on the parameter axis for arbitrary periodic words $\mathbf{W}$ and $\mathbf{Q}$. Because of the property of accumulation and contraction of $*$ operation [5,6], the norm $|\,|$ will be contracted with the word changing from $\mathbf{W}_{1,2}$ to $\mathbf{Q}*\mathbf{W}_{1,2}$ and simultaneously with the increasing of the length of word, so we always have $\eta(\mathbf{Q})<1$; thus (1.1) reflects the compression effect of $\mathbf{Q}*$ operation in the λ parameter space. For the quadratic map $f_\lambda(x)=1-\lambda x^2$, $\eta(\mathbf{Q})$ takes the simple form

$$\eta(\mathbf{Q})=\delta^{-1}(\mathbf{Q}) \qquad (1.2)$$

with a high precision. Because of the simplicity of (1.2), we will take the quadratic map $f_\lambda(x)=1-\lambda x^2$ as the actual metric model in this paper.

The devil's staircase of topological entropy indicates that there are two important intervals: one is of zero entropy corresponding to the main period-doubling bifurcation (PDB) cascade sequences $R*^n$ and the other is of nonzero entropy corresponding to other sequences except $R*^n$. Our research here indicates further that in these intervals there still exist the following three kinds of characteristic intervals and their corresponding global scaling phenomena: (i) the periodic window $l_W(\mathbf{Q})$, (ii) the window band $l_{\rm WB}(\mathbf{Q})$, and (iii) the ETEC step $l_h(\mathbf{Q})$. Each of these three characteristic intervals is formed by the same topological conjugate compression operation $\mathbf{Q}*$, but for the different characteristic boundary sequences. Thus we will have a series of characteristic constants to describe the global scaling behaviors. Among these characteristic constants, the ETEC step scaling constant $\mu_c=\frac{9}{4}$ should be emphasized, which is just *the normalized crisis*

*Mailing address: Department of Physics, Yunnan Institute of the Nationalities, Kunming, Yunnan 650031, China.

value of ''windows'' found by Yorke, Grebogi, Ott, and Tedeschini-Lalli [8]; however, at that time, they did not give an accurate interpretation; we will present the clear geometric meaning. We also obtain two different window scaling ratios, i.e., $\gamma_{\rm PDB}=1$ for the PDB cascade sequences and $\gamma_N=\frac{1}{3}$ for the non-PDB sequences, which determine the universal positions of superstable points in all the periodic windows. These scaling constants fully reflect the property of the uniform compression of $\mathbf{Q}*$ operation on the whole parameter axis.

As an interesting result of the uniform compression, the width l_W of the periodic window is proportional to the compression ratio δ^{-1}, the reciprocal of the convergent rate; for some specific maps such as the quadratic map, l_W can even be normalized to unity by δ^{-1}. This is an important global scaling phenomenon, which leads to a significant and analytic formula: the chaotic measure describing the irregularity highly unifies the universal convergent rates describing the periodic regularity. This is the final aim of this paper; it provides analytic evidence for the problem that chaos has a positive measure [9,10].

In this paper we will first introduce the notation and some basic concepts in Sec. II. In Sec. III we discuss the global scaling behaviors and present the universality for the positions of the superstable points in all the periodic windows. In Sec. IV the approximate analytic formula of the chaotic measure is obtained by employing the convergent rates of the periodic sequences. In Sec. V we calculate the singularity spectrum and the generalized fractal dimension of the chaotic set, which are improved compared to those in Ref. [4]. Finally, in Sec. VI we give a short discussion.

II. NOTATION AND BASIC CONCEPTIONS

A. DGP * composition rule and ETEC

From the symbolic dynamics [10–12] it is known that an orbit can be described by a kneading symbolic sequence (word) $\mathbf{K}=K_1K_2\cdots K_k\cdots$:

$$K_i=\begin{cases} L \\ C \\ R \end{cases} \quad \text{for } f_\lambda^i \begin{cases} <0 \\ =0 \\ >0, \end{cases} \quad i=1,2,\ldots,k,\ldots. \tag{2.1}$$

As a convention, an aperiodic sequence of infinite length is usually called an infinite word, while a periodic sequence $\mathbf{K}=(K_1K_2\cdots K_k)^\infty$ of period k, with the repeating byte $K_1K_2\cdots K_k$ of finite length as its characteristic, is called a finite word, which is usually represented by its repeating byte, i.e., $\mathbf{K}=K_1K_2\cdots K_k$. In particular, a periodic sequence with a symbol C is referred to as a superstable periodic sequence (word) [10] or Metropolis-Stein-Stein (MSS) sequence [11].

Now we introduce the DGP * composition rule [5]. Let two superstable periodic sequences be $\mathbf{Q}=Q_1Q_2\cdots Q_qC$ and $\mathbf{S}=S_1S_2\cdots S_sC$. Then the ith symbol P_i of the compound sequence $\mathbf{P}=\mathbf{Q}*\mathbf{S}$ can be written as [13]

$$P_i=\begin{cases} Q_j & \text{if } i \bmod (q+1)=j\neq 0 \\ S_k^{t(\mathbf{Q})} & \text{if } i=k(q+1) \\ C & \text{if } i=(q+1)(s+1), \end{cases} \tag{2.2}$$

where t is the parity inverse operator defined by $L^t=R$, $R^t=L$, and $t(\mathbf{Q})=t^{J(\mathbf{Q})}$, with $J(\mathbf{Q})$ the R-parity number of sequence $\mathbf{Q}$ (the number of appearances of the symbol R in $\mathbf{Q}$). It is obvious that $t^{2n+1}=t$, $t^{2n}=I$; here I denotes the identity operator.

In Refs. [2] and [3] we have proved that the DGP composition $\mathbf{Q}*$ of arbitrary superstable periodic sequences (MSS sequences) is a topological conjugate operation that preserves the topological entropy; namely, independent of whatever $\mathbf{W}$ is ($\mathbf{W}\in\mathcal{W}$, the set of all admissible sequences with the minimal L^∞ and the maximal RL^∞), an ETEC $\mathbf{Q}*\mathcal{W}\equiv\{\mathbf{Q}*\mathbf{W}|\mathbf{W}\in\mathcal{W}\}$ is formed under this operation, with a constant topological entropy $h(\mathbf{Q})$. We have also obtained that the composition operator $\mathbf{Q}*$ compresses the space $[L^\infty,RL^\infty]$ of all admissible sequences to an ETEC that exhibits a step in the entropy plot $h-\lambda$, with the width (Lebesgue measure) $l_h(\mathbf{Q})=|\mathbf{Q}*[L^\infty,RL^\infty]|$.

B. Periodic window and convergent rate

We call such three periodic sequences $(\mathbf{A}L^{t(\mathbf{A})},\mathbf{A}C,\mathbf{A}R^{t(\mathbf{A})})$ in the ascending order a periodic window labeled by $\mathbf{A}$, where $\mathbf{A}C\equiv(\mathbf{A}C)^\infty$ denotes the superstable periodic sequence and $\mathbf{A}L^{t(\mathbf{A})}\equiv(\mathbf{A}L^{t(\mathbf{A})})^\infty=\mathbf{A}*L^\infty$ and $\mathbf{A}R^{t(\mathbf{A})}\equiv(\mathbf{A}R^{t(\mathbf{A})})^\infty=\mathbf{A}*R^\infty$ are called the lower and the upper sequences [12,14] of $\mathbf{A}C$, respectively. On the parameter axis, the parameter values corresponding to the window sequences are denoted by $(\lambda_l,\lambda_c,\lambda_r)$. As both the lower and the upper sequences correspond to the parameter intervals, from now on we shall specially denote λ_l and λ_r as the parameter values of the left and the right boundaries of the window that satisfy the stability condition $|\Pi_i f_\lambda'(x_i)|=1$. Thus the width of the periodic window of sequence $\mathbf{A}$ on the parameter axis is

$$\begin{aligned} l_W(\mathbf{A})&=|[\mathbf{A}L^{t(\mathbf{A})},\mathbf{A}R^{t(\mathbf{A})}]|=|\mathbf{A}*[L^\infty,R^\infty]| \\ &\equiv\lambda_r(\mathbf{A})-\lambda_l(\mathbf{A}). \end{aligned} \tag{2.3}$$

For the period-p-tupling bifurcation sequence $\mathbf{A}^{*n}$ (p is the period of $\mathbf{A}$) [12,15], it is well known that the widths of adjacent windows, or the distances between the superstable points, form the universal convergent rate $\delta(\mathbf{A})$ for any one-dimensional maps of quadratic maximum, i.e.,

$$\delta(\mathbf{A})=\lim_{n\to\infty}\frac{l_W(\mathbf{A}^{*n})}{l_W(\mathbf{A}^{*(n+1)})}=\lim_{n\to\infty}\frac{\lambda_r(\mathbf{A}^{*n})-\lambda_l(\mathbf{A}^{*n})}{\lambda_r(\mathbf{A}^{*(n+1)})-\lambda_l(\mathbf{A}^{*(n+1)})} \tag{2.4}$$

or

$$\delta(\mathbf{A})=\lim_{n\to\infty}\frac{\lambda_c(\mathbf{A}^{*(n+1)})-\lambda_c(\mathbf{A}^{*n})}{\lambda_c(\mathbf{A}^{*(n+2)})-\lambda_c(\mathbf{A}^{*(n+1)})}. \tag{2.5}$$

The two definitions (2.4) and (2.5) are equivalent in the numerical calculations. They are not only two convergent subsequences that approach the same accumulation point $\lambda(\mathbf{A}^{*\infty})$, as told by Feigenbaum [1], Hao [12], and Chang and McCown [15], but also the important result of uniform compression. In the numerical calculations, (2.5) is more convenient because λ_c is very easy to compute by the word-lifting technique [12].

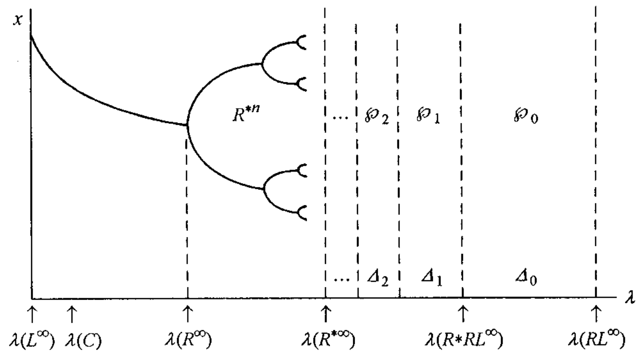

FIG. 1. Schematic diagram for the self-similar classification of the basic sequences.

C. Window band

The window band of sequence **A** refers to the total of the windows of **A** and all the associated Feigenbaum (PDB cascade) sequences of the form $\mathbf{A}*R^{*n}$ with $n=1,2,\ldots$. These windows are connected on the parameter axis, which means that the upper sequence of any window in the window band coincides with the lower sequence of the next adjacent window, leaving no room for other sequences to get in between, i.e., $\lambda_r(\mathbf{A}*R^{*n})=\lambda_l(\mathbf{A}*R^{*(n+1)})$ holds from (2.3). The window band is the result that the operation $\mathbf{A}*$ compresses the whole connected region of the main PDB cascade R^{*n} into the chaotic region. Noting that the sequences $\mathbf{A}*R^{*n}$ have the same convergent rate $\delta(R)=4.66920\cdots$ as the main PDB sequences R^{*n} [16,17], i.e., $l_W(\mathbf{A}*R^{*n})/l_W(\mathbf{A}*R^{*(n+1)})\to\delta(R)$, therefore, on the parameter axis, the width of the window band is

$$l_{\mathrm{WB}}(\mathbf{A})=\sum_{n=0}^{\infty} l_W(\mathbf{A}*R^{*n})=|\mathbf{A}*[L^{\infty},R^{*\infty}]|$$
$$\approx l_W(\mathbf{A})\sum_{n=0}^{\infty}\delta^{-n}(R)=\frac{l_W(\mathbf{A})}{1-\delta^{-1}(R)}. \qquad (2.6)$$

The width l_{WB} of the window band will play an important role later in the calculation of the chaotic measure.

D. Self-similar structure in the chaotic region

To compute the chaotic measure in Sec. IV we need to study the total width L_{WB}^{t} of all the periodic windows (window bands). This requires the knowledge about the structure of the chaotic region.

In the bifurcation diagram, we can classify the *basic* periodic and quasiperiodic sequences in Fig. 1 according to the MSS order [11] and the structural similarity of sequences. The chaotic region $\Delta_c=[R^{*\infty},RL^{\infty}]$ can be divided into a series of subintervals $\Delta_m=[R^{*(m+1)}*RL^{\infty},R^{*m}*RL^{\infty}]$ ($m=0,1,2,\ldots$); the set of the basic periodic and quasiperiodic sequences corresponding to each subinterval Δ_m is denoted as $\wp_m$. The widths of subintervals are obviously the convergent series $|\Delta_0|,|\Delta_1|,|\Delta_2|,\ldots,|\Delta_m|,\ldots$ satisfying $\lim_{m\to\infty}|\Delta_m|/|\Delta_{m+1}|=\delta(R)$.

The MSS primitive words that cannot be decomposed by the DGP $*$ composition rule are of most significance for our calculation. The set of all primitive words of period greater than or equal to 3 is denoted by $\wp_\pi$. All these primitive words are located in the subinterval Δ_0. Except the primitive words, there are also the compound sequences (words) of the form $\mathbf{Q}_1*R^{*n_1}*\cdots*\mathbf{Q}_k*R^{*n_k}*\mathbf{Q}_{k+1}$ in Δ_0; thus

$$\wp_0=\{\mathbf{Q},\mathbf{Q}_1*R^{*n_1}*\cdots*\mathbf{Q}_k*R^{*n_k}*\mathbf{Q}_{k+1}|\mathbf{Q}\in\wp_\pi,\mathbf{Q}_k\in\wp_\pi;$$
$$k\geqslant 1,\ n_k\in\mathbb{Z}^+\}, \qquad (2.7)$$

where $\mathbb{Z}^+$ is the set of positive integers. Obviously, the various possible combinations, such as $\mathbf{Q}^{*j}$, $\mathbf{Q}_1^{*j_1}*R^{*n_1}*\cdots*\mathbf{Q}_k^{*j_k}$, are included in $\wp_0$. It should be indicated that though there are also the associated Feigenbaum PDB sequences $\mathbf{A}*R^{*n}$ ($\mathbf{A}\in\wp_0$, $n\geqslant 1$) in the subinterval Δ_0, we do not include them in $\wp_0$ since we only need the basic sequences **A** to calculate the window band sequences $\mathbf{A}*R^{*n}$ from (2.6). For other subintervals Δ_m with $m\geqslant 1$, we have

$$\wp_m=R^{*m}*\wp_0. \qquad (2.8)$$

Therefore, the set of all the basic MSS sequences (periodic and quasiperiodic) except the main PDB sequences R^{*n} and the associated PDB sequences $\mathbf{A}*R^{*n}$ is

$$\wp=\bigcup_{m=0}^{\infty}\wp_m. \qquad (2.9)$$

The structure of each subinterval Δ_m is completely similar and the cardinal of each set $\wp_m$ is also the same. The difference between $\wp_{m+1}$ and $\wp_m$ is only a compression map $R*$. So when considering the chaotic measure we shall concentrate mainly on the treatment of the set $\wp_0$ in Δ_0; other sets $\wp_m$ in Δ_m ($m\geqslant 1$) can be treated immediately from the similarity.

III. GLOBAL SCALING BEHAVIORS AND UNIVERSAL SUPERSTABLE POSITIONS IN PERIODIC WINDOWS

A. Window-δ relation

We know from (2.3) and (2.4) that the definitions for the window widths $l_W(\mathbf{Q})$ of the periodic sequences **Q** and the convergent rates $\delta(\mathbf{Q})$ of the period-p-tupling bifurcations $\mathbf{Q}^{*n}$ are, respectively,

$$l_W(\mathbf{Q})=|\mathbf{Q}*[L^{\infty},R^{\infty}]|=\eta(\mathbf{Q})|[L^{\infty},R^{\infty}]|,$$

$$\delta(\mathbf{Q})=\lim_{n\to\infty}\frac{|\mathbf{Q}^{*n}*[L^{\infty},R^{\infty}]|}{|\mathbf{Q}^{*(n+1)}*[L^{\infty},R^{\infty}]|}.$$

Through the numerical calculation for the quadratic map $f_\lambda(x)=1-\lambda x^2$, we find that there exists a very simple inverse proportion relation between them (see Table I), i.e.,

$$l_W(\mathbf{Q})=\delta^{-1}(\mathbf{Q}), \qquad (3.1)$$

which holds approximately with at least two significant figures. This implies the important concept that the DGP composition $\mathbf{Q}*$ for any sequence **Q** is a compression operation [3] with the uniform compression ratio $\delta^{-1}(\mathbf{Q})$. It will play an important role in the calculation of the chaotic measure. The relation (3.1) is consistent with (1.1), because from

TABLE I. Numerical data of $\delta^{-1}(\mathbf{Q})$, $l_W(\mathbf{Q})$, and the relative deviation of $\delta^{-1}(\mathbf{Q})$ from $l_W(\mathbf{Q})$, for the MSS primitive words $\mathbf{Q}$ of period $p=3$–7. In the calculation, the width of periodic window $l_W(\mathbf{Q})$ and the convergent rate $\delta(\mathbf{Q})$ are, respectively, computed from (2.3) and (2.5) for the quadratic map $f_\lambda(x)=1-\lambda x^2$.

p	$\mathbf{Q}$	$\delta^{-1}(\mathbf{Q})$	$l_W(\mathbf{Q})$	$\lvert l_W-\delta^{-1}\rvert/l_W$
3	*RL*	0.018 100 521 6	0.018 529 152 5	0.023
4	*RLL*	0.001 018 750 1	0.000 986 964 3	0.032
5	*RLRR*	0.003 913 201 2	0.004 038 761 4	0.031
5	*RLLR*	0.000 776 953 0	0.000 778 122 8	0.001 5
5	*RLLL*	0.000 059 064 5	0.000 058 128 2	0.016
6	*RLLRR*	0.000 117 539 5	0.000 117 572 3	0.000 28
6	*RLLLR*	0.000 035 684 1	0.000 035 599 0	0.002 4
6	*RLLLL*	0.000 003 582 6	0.000 003 561 5	0.005 9
7	*RLRRRR*	0.000 691 352 0	0.000 694 609 3	0.004 7
7	*RLRRLR*	0.000 443 696 6	0.000 447 198 5	0.007 8
7	*RLLRLR*	0.000 098 332 1	0.000 098 482 9	0.001 5
7	*RLLRRR*	0.000 043 782 1	0.000 043 798 4	0.000 37
7	*RLLRRL*	0.000 028 324 0	0.000 028 391 9	0.002 4
7	*RLLLRL*	0.000 015 716 1	0.000 015 689 9	0.001 7
7	*RLLLRR*	0.000 005 982 2	0.000 005 978 8	0.000 57
7	*RLLLLR*	0.000 002 051 9	0.000 002 049 7	0.001 1
7	*RLLLLL*	0.000 000 221 6	0.000 000 221 2	0.001 8

(1.1), $l_W(\mathbf{Q})=\delta^{-1}(\mathbf{Q})\lvert[L^\infty,R^\infty]\rvert$, while $\lambda(L^\infty)=-\frac{1}{4}$ and $\lambda(R^\infty)=\frac{3}{4}$ results in that $\lvert[L^\infty,R^\infty]\rvert=1$. If we rewrite (3.1) into the form

$$l_W(\mathbf{Q})\,\delta(\mathbf{Q})=1, \tag{3.1$'$}$$

then we can see the obvious scaling effect of $\delta^{-1}(\mathbf{Q})$. Obviously, it is a global relationship independent of the sequences $\mathbf{Q}$.

For the compound sequences, there is the general approximation $\delta(\mathbf{Q}_1*\mathbf{Q}_2)\approx\delta(\mathbf{Q}_1)\delta(\mathbf{Q}_2)$ [6], so we have

$$l_W(\mathbf{Q}_1*\mathbf{Q}_2)\approx\delta^{-1}(\mathbf{Q}_1)\,\delta^{-1}(\mathbf{Q}_2). \tag{3.2}$$

It should be noted that $\delta(R*^n*\mathbf{Q})\approx\delta^n(R)\delta(\mathbf{Q})$ holds for large n; however, it does not work well for $n=1$. We will consider the corrections for this in Sec. IV.

B. Scaling behaviors of window bands

1. Scaling coefficient K_f for the window band

From (2.6) and (3.1) the width of the window band can be written as

$$l_{\mathrm{WB}}(\mathbf{Q})=\delta^{-1}(\mathbf{Q})\lvert[L^\infty,R*^\infty]\rvert\equiv K_f\delta^{-1}(\mathbf{Q}), \tag{3.3}$$

where the *theoretical* value of the coefficient $K_f=1.651\,15\cdots$ because $\lambda(L^\infty)=-0.25$ and $\lambda(R*^\infty)=1.401\,15\cdots$. Using the approximation in (2.6), we can also express $l_{\mathrm{WB}}(\mathbf{Q})$ as

$$l_{\mathrm{WB}}(\mathbf{Q})\approx\frac{\delta^{-1}(\mathbf{Q})}{1-\delta^{-1}(R)}. \tag{3.4}$$

Of these two expressions, (3.3) is more accurate than (3.4). Here we show how to give $l_{\mathrm{WB}}(\mathbf{Q})$ with merely the convergent rates in (3.4). The approximate expression (3.4) implies that $1/[1-\delta^{-1}(R)]=1.272\,53\cdots$, which is considerably different from K_f in (3.3) because $l_W(\mathbf{Q})/l_W(\mathbf{Q}*R)\approx2$ [see $\delta_1(R)$ in Table V] has a large deviation from $\delta(R)$, which will be improved in Sec. IV. Therefore, $1/[1-\delta^{-1}(R)]=1.272\,53\cdots$ is an *ideal* value of K_f, which requires the uniform convergence of the forward PDB sequences $\mathbf{Q}*R*^n$, i.e., $l_W(\mathbf{Q}*R*^n)/l_W(\mathbf{Q}*R*^{(n+1)})=\delta(R)$ strictly holds for each n $(=0,1,2,\ldots)$.

We can rewrite (3.3) as

$$l_{\mathrm{WB}}(\mathbf{Q})\,\delta(\mathbf{Q})=K_f, \tag{3.3$'$}$$

which shows again the scaling effect of $\delta^{-1}(\mathbf{Q})$ as in (3.1′). This is also a global relationship independent of the sequences $\mathbf{Q}$.

2. Scaling coefficient K_b for the total width of all window bands

We now calculate the total width $L^t_{\mathrm{WB}}=\Sigma_{\mathbf{A}\in\wp}l_{\mathrm{WB}}(\mathbf{A})$ of all window bands in the chaotic region, which is the key point for computing the chaotic measure. Here the summation should take over all the possible combinations (the primitive words and their various combinations with $R*^{n_k}$). Due to the self-similar structure of the chaotic region, we can express L^t_{WB} in the following form, according to the classification in Sec. II D:

$$L^t_{\mathrm{WB}}=\sum_{m=0}^{\infty}L_{\mathrm{WB},m}, \tag{3.5}$$

where $L_{\mathrm{WB},m}$ is the sum of the widths of all window bands in the subinterval Δ_m. Once the sum $L_{\mathrm{WB},0}$ in the subinterval Δ_0 is found, then $L_{\mathrm{WB},m}$ in other subintervals Δ_m can be obtained immediately from the similarity.

Calculating $L_{\mathrm{WB},0}\equiv\Sigma_{\mathbf{A}\in\wp_0}l_{\mathrm{WB}}(\mathbf{A})$ in Δ_0, first, taking $\mathbf{A}=\mathbf{Q}\in\wp_\pi$, we have, from (3.4),

$$B_1\equiv\sum_{\mathbf{Q}\in\wp_\pi}l_{\mathrm{WB}}(\mathbf{Q})\approx\frac{1}{1-\delta^{-1}(R)}\sum_{\mathbf{Q}\in\wp_\pi}\delta^{-1}(\mathbf{Q})<1. \tag{3.6}$$

Here we expect to calculate L^t_{WB} with merely the convergent rates; the corrections will be considered in Sec. IV. Second, taking $\mathbf{A}=\mathbf{Q}_1*R*^{n_1}*\mathbf{Q}_2$ with $\mathbf{Q}_1$, $\mathbf{Q}_2\in\wp_\pi$, then from (3.4) and (3.2) we have

$$\begin{aligned}B_2&\equiv\sum_{\mathbf{Q}_1\in\wp_\pi}\sum_{\mathbf{Q}_2\in\wp_\pi}\sum_{n_1\in\mathbb{Z}^+}l_{\mathrm{WB}}(\mathbf{Q}_1*R*^{n_1}*\mathbf{Q}_2)\\&\approx\left[\frac{1}{1-\delta^{-1}(R)}\right]^2\sum_{\mathbf{Q}_1\in\wp_\pi}\sum_{\mathbf{Q}_2\in\wp_\pi}\delta^{-1}(\mathbf{Q}_1)\,\delta^{-1}(\mathbf{Q}_2)=B_1^2.\end{aligned} \tag{3.7}$$

Third, by induction, and noting that $B_1<1$ in (3.6) guarantees convergence of the geometric series, we obtain

$$\begin{aligned}L_{\mathrm{WB},0}&\equiv\sum_{\mathbf{A}\in\wp_0}l_{\mathrm{WB}}(\mathbf{A})=B_1+B_2+\cdots+B_k+\cdots\\&\approx B_1+B_1^2+\cdots+B_1^k+\cdots=\frac{B_1}{1-B_1}.\end{aligned} \tag{3.8}$$

Calculating $L_{\mathrm{WB},m}$ in the subinterval Δ_m, from (2.8) we have

$$L_{\mathrm{WB},m} \equiv \sum_{\mathbf{A}\in\wp_m} l_{\mathrm{WB}}(\mathbf{A}) = L_{\mathrm{WB},0}/\delta^m(R). \tag{3.9}$$

Summing up the results over each subinterval, one can obtain finally

$$L^t_{\mathrm{WB}} = \sum_{m=0}^{\infty} L_{\mathrm{WB},m} = \frac{L_{\mathrm{WB},0}}{1-\delta^{-1}(R)} \equiv K_b L_{\mathrm{WB},0}, \tag{3.10}$$

where the scaling coefficient $K_b = 1/[1-\delta^{-1}(R)] = 1.272\,53\cdots$. This value of K_b is an *ideal* value, which requires the uniform convergence of the backward (reversed) PDB sequences $R^{*m}*\mathbf{Q}$, i.e., $l_W(R^{*m}*\mathbf{Q})/l_W(R^{*(m+1)}*\mathbf{Q}) = \delta(R)$ strictly holds for each m $(=0,1,2,\cdots)$.

C. Geometric interpretation for the YGOTL's scaling constant μ_c

Yorke, Grebogi, Ott, and Tedeschini-Lalli (YGOTL) pointed out in Ref. [8] the scaling behavior of ''windows'' in the one-dimensional maps, which has not yet been fully understood since then. The width of the ''window'' in that paper is exactly the width of the ETEC step found by us [2–4]

$$l_h(\mathbf{Q}) = |\mathbf{Q}*[L^\infty, RL^\infty]| = \lambda(\mathbf{Q}*RL^\infty) - \lambda(\mathbf{Q}L^{t(\mathbf{Q})}). \tag{3.11}$$

Inside the ETEC step, however, there are various window bands l_{WB}. There are also the single points corresponding to a coarse-grained chaotic set such as $\mathbf{Q}*\wp_{\mathrm{chaos}}$ (where $\wp_{\mathrm{chaos}}$ is the set of the chaotic sequences). According to YGOTL, the normalized crisis value of ''windows'' in Ref. [8] is

$$\mu_c = \frac{l_h(\mathbf{Q})}{l_W(\mathbf{Q})} = \frac{|\mathbf{Q}*[L^\infty, RL^\infty]|}{|\mathbf{Q}*[L^\infty, R^\infty]|} = \frac{9}{4}. \tag{3.12}$$

The last equality holds within an accuracy of $\pm 3\%$ [8]. This value $\frac{9}{4}$ can be derived from the uniform compressibility of the operator $\mathbf{Q}*$ [3]. For the quadratic map, $\lambda(L^\infty) = -\frac{1}{4}$, $\lambda(R^\infty) = \frac{3}{4}$, and $\lambda(RL^\infty) = 2$; thus, combining (1.1) and (1.2) we can easily have

$$\mu_c = \frac{|[L^\infty, RL^\infty]|}{|[L^\infty, R^\infty]|} = \frac{9}{4}. \tag{3.12$'$}$$

From (3.12′) we give a very clear geometric interpretation of YGOTL's scaling constant $\frac{9}{4}$, namely, it is a result of the uniform compression of $\mathbf{Q}*$ operation preserving the topological entropy.

Moreover, from (3.1) and (3.12), a universal relation

$$l_h(\mathbf{Q})\,\delta(\mathbf{Q}) = \tfrac{9}{4} \tag{3.13}$$

approximately holds with at least two significant figures, which is independent of the sequences $\mathbf{Q}$. Because of (3.13), μ_c can also be thought as the ETEC step scaling constant. From (3.13), together with (3.1′) and (3.3′), namely, $l_W(\mathbf{Q})\delta(\mathbf{Q}) = 1$ and $l_{\mathrm{WB}}(\mathbf{Q})\delta(\mathbf{Q}) = K_f$, we can see the obvious compression effect of $\delta^{-1}(\mathbf{Q})$, as $\mathbf{Q}*$ is a compression operation. These three relationships clearly show that if we take $\delta^{-1}(\mathbf{Q})$ as a scaling length, then for any sequences $\mathbf{Q}$, whatever the ETEC steps $l_h(\mathbf{Q})$, the periodic windows $l_W(\mathbf{Q})$, or the window bands $l_{\mathrm{WB}}(\mathbf{Q})$, all can be scaled as constants respectively.

TABLE II. Window scaling ratio $\gamma_{\mathrm{PDB}} = (\lambda_c - \lambda_l)/(\lambda_r - \lambda_c)$ of the PDB sequences $(\mathbf{A}*)R^{*n}$ is universal for different sequences $\mathbf{A}$. These values are obtained from the calculation on R^{*n} for the quadratic map. The last column gives the relative deviation of γ_{PDB} from 1.

n	γ_{PDB}	$\lvert\gamma_{\mathrm{PDB}}-1\rvert$
1	1	0
2	1.057 605 51	0.058
3	1.075 997 90	0.076
4	1.079 424 25	0.079
5	1.080 222 86	0.080
6	1.080 386 00	0.080
7	1.080 421 92	0.080
8	1.080 429 49	0.080

D. Universality for the positions of superstable points in periodic windows

1. Universal window scaling ratio $\gamma_{PDB}=1$ for the PDB cascade sequences

The PDB cascade sequences include the main PDB sequences R^{*n} and their compressions $\mathbf{A}*R^{*n}$ ($n\geq 1$, $\mathbf{A}\in\wp$; see Sec. II D for the definition of $\wp$). One of the characteristics of the PDB sequences is that they have connected windows in the bifurcation diagram, i.e., $\lambda_r(\mathbf{A}*R^{*n}) = \lambda_l(\mathbf{A}*R^{*(n+1)})$. For this type of sequence, we find that in the periodic windows $(\lambda_l, \lambda_c, \lambda_r)$ of any value of n (≥ 1), the ratio for the widths of the stable regions on both sides of the superstable points

$$\gamma_{\mathrm{PDB}}(n) = \frac{\lambda_c - \lambda_l}{\lambda_r - \lambda_c} = \frac{|R^{*n}*[L^\infty, C]|}{|R^{*n}*[C, R^\infty]|} \text{ or } \frac{|\mathbf{A}*R^{*n}*[L^\infty, C]|}{|\mathbf{A}*R^{*n}*[C, R^\infty]|} \tag{3.14}$$

is independent of the sequences $\mathbf{A}$ (i.e., universal for $\mathbf{A}$). Noting that R^{*n} is the zero topological entropy class [2–4], its representative is the period-2 window $R*[L^\infty, R^\infty]$ ($n=1$); other cascade periodic windows $R^{*n}*[L^\infty, R^\infty]$ ($n\geq 2$) are the compressions of the typical period-2 window. For the quadratic map $\lambda(RR) = \lambda(R^\infty) = \frac{3}{4}$, $\lambda(RC) = 1$, and $\lambda(RL) = \frac{5}{4}$; thus we have, from (3.14),

$$\gamma_{\mathrm{PDB}} = \frac{|R*[L^\infty, C]|}{|R*[C, R^\infty]|} = \frac{|[RR, RC]|}{|[RC, RL]|} = 1. \tag{3.14$'$}$$

The ratio $\gamma_{\mathrm{PDB}} = 1$ is within an accuracy of $\pm 8\%$ and has been verified by the numerical calculation (see Table II). However, we can see that $\gamma_{\mathrm{PDB}}(n)$ values have some minor numerical deviations from (3.14′), i.e., $\gamma_{\mathrm{PDB}}(n)$ slightly depends on n, which comes from the fact that $l_W(R^{*n})/l_W(R^{*(n+1)}) \approx \delta(R)$ (not strictly =). This interesting universal scaling ratio γ_{PDB} originates from the uniform compression of R^{*n}.

TABLE III. Numerical result for the window scaling ratio $\gamma_N=(\lambda_c-\lambda_l)/(\lambda_r-\lambda_c)$ of the non-PDB sequences. Here we show only the values for the MSS primitive words **Q** of period $p=3$–7 as examples. The last column gives the relative deviation of γ_N from $\frac{1}{3}$.

p	**Q**	γ_N	$\lvert\gamma_N-\frac{1}{3}\rvert/(\frac{1}{3})$
3	RL	0.357 299 28	0.072
4	RLL	0.337 446 51	0.012
5	$RLRR$	0.336 441 89	0.009 3
5	$RLLR$	0.335 663 97	0.007 0
5	$RLLL$	0.334 247 21	0.002 7
6	$RLLRR$	0.333 636 36	0.000 91
6	$RLLLR$	0.333 620 44	0.000 86
6	$RLLLL$	0.333 553 67	0.000 66
7	$RLRRRR$	0.332 777 63	0.001 7
7	$RLRRLR$	0.334 453 67	0.003 4
7	$RLLRLR$	0.333 625 70	0.000 88
7	$RLLRRR$	0.333 555 14	0.000 67
7	$RLLRRL$	0.333 225 63	0.000 32
7	$RLLLRL$	0.333 551 00	0.000 65
7	$RLLLRR$	0.333 392 90	0.000 18
7	$RLLLLR$	0.333 391 91	0.000 18
7	$RLLLLL$	0.333 387 83	0.000 16

2. Universal window scaling ratio $\gamma_N=\frac{1}{3}$ for the non-PDB sequences

For other periodic sequences that are not the PDB cascade sequences, namely, the sequences that cannot be decomposed as being multiplied by R^{*n} from the right, i.e., $\mathbf{A}\in\wp$ but $\mathbf{A}\neq\mathbf{A}'*R^{*n}$ (e.g., $\mathbf{A}=\mathbf{Q}$, $\mathbf{Q}_1*R^{*n_1}*\cdots*\mathbf{Q}_k$, $R^{*m}*\mathbf{Q}$), we can still define the ratio

$$\gamma_N(\mathbf{A})=\frac{\lambda_c(\mathbf{A})-\lambda_l(\mathbf{A})}{\lambda_r(\mathbf{A})-\lambda_c(\mathbf{A})}=\frac{|\mathbf{A}*[L^\infty,C]|}{|\mathbf{A}*[C,R^\infty]|}. \qquad (3.15)$$

On the basis of the compressibility of the operation $\mathbf{A}*$ and noting that $\lambda(C)=0$ for the quadratic map, we thus have, from (1.1) and (3.15),

$$\gamma_N=\frac{|[L^\infty,C]|}{|[C,R^\infty]|}=\frac{1}{3}. \qquad (3.15')$$

The ratio $\gamma_N=\frac{1}{3}$ is within an accuracy of $\pm7\%$ and has been numerically verified. From Table III we can see that the maximal deviation 7% occurs at the period-3 primitive word RL, while the deviation for other primitive words is much smaller than this. Similarly, the maximal deviation for YGOTL's constant μ_c also occurs at the same word RL [8]. The Table III data imply that the deviation tends to be smaller as the period p and the parameter λ of the word increase. The γ_N is an interesting universal scaling ratio that does not depend on the sequences **A**, which is very useful in practice. For example, when calculating the periodic window of a sequence **A** of very large period with a computer, one often encounters difficulty in solving $\lambda_l(\mathbf{A})$ and $\lambda_r(\mathbf{A})$ numerically; however, with the aid of (3.15′), one can easily obtain the boundaries of the window from the superstable point $\lambda_c(\mathbf{A})$ and the convergent rate $\delta(\mathbf{A})$ as

$$\lambda_l(\mathbf{A})=\lambda_c(\mathbf{A})-\frac{1}{4}\,l_W(\mathbf{A})=\lambda_c(\mathbf{A})-\frac{1}{4\,\delta(\mathbf{A})},$$
$$\lambda_r(\mathbf{A})=\lambda_c(\mathbf{A})+\frac{3}{4}\,l_W(\mathbf{A})=\lambda_c(\mathbf{A})+\frac{3}{4\,\delta(\mathbf{A})}. \qquad (3.16)$$

In this section we have presented a series of global scaling constants, such as μ_c, $\gamma_{\rm PDB}$, and γ_N, that do not depend on the sequences.

IV. CHAOTIC MEASURE AS THE FUNCTION OF THE CONVERGENT RATES OF PERIOD-*P*-TUPLING BIFURCATIONS

A. Strategy: Describing chaos by periodicity

Periodic motion and aperiodic chaotic motion are two different kinds of motion. Today there is a very deep understanding and universal quantitative description for periodic motion [1,5,10–13,15]; however, this is not the case for the aperiodic chaotic orbits. Here we take the global result of the metric universality as our starting point. The periodic sequences and the aperiodic sequences form a whole body. The knowledge of the universality of periodic sequences can help us realize and understand the behavior of aperiodic sequences. The strategy of this section is to take both sequences as two sides of the whole body; thus we can calculate one from another.

In Ref. [3] we suggested a classification of all admissible sequences (words) in the complete topological space Σ_2 of two symbols. All the admissible sequences can be divided into two large classes: (i) regular periodic sequences and (ii) aperiodic chaotic sequences, which include the coarse-grained chaotic sequences of infinite length generated by limited grammatical rules (such as the eventually periodic sequences, $\mathbf{AB}^\infty$-type sequences [18], $\boldsymbol{\rho\lambda}^\infty$-type kneading sequences [19,20], and the infinite limits of Fibonacci sequences [21]) and the Bernoulli-Chaitin-Ford infinite sequences [22,23] that cannot be generated by limited grammatical rules and are the fine-grained chaos in the sense of symbolic dynamics.

There is an important question of how the chaotic orbits (sequences) distribute on the parameter axis λ and what the chaotic measure is. Jakobson [9] proved that there is positive measure for chaos. Then Wang and Chen [24] employed the Monte Carlo method on the logistic model with the positive Lyapunov exponent as a criterion to make a statistical sampling and estimated the chaotic measure to be $\mathcal{L}_c=0.893\pm0.022$ (the total measure of chaotic region is normalized to unity), which shows that the measure of chaotic orbits (sequences) in the chaotic region is greater than that of periodic orbits (sequences).

As we have seen in the above, the periodic sequences have windows whose distributions on the parameter axis λ form intervals, while this does not hold for the chaotic sequences. The chaotic sequences are the single points on the parameter axis λ. Thus we shall obtain chaos by excluding all the infinitely many periodic windows (or window bands) in the chaotic region Δ_c, i.e., the complementary set to all the window bands represents chaos both in the coarse-grain

TABLE IV. Numerical results of $\Sigma\delta^{-1}(\mathbf{Q})$, $\Sigma l_W(\mathbf{Q})$, and the relative deviation of $\Sigma\delta^{-1}(\mathbf{Q})$ from $\Sigma l_W(\mathbf{Q})$, for the MSS primitive words of period $p=3$–14. N denotes the number of the primitive words (windows) calculated.

p	N	$\Sigma\delta^{-1}(\mathbf{Q})$	$\Sigma l_W(\mathbf{Q})$	$\lvert\Sigma l_W-\Sigma\delta^{-1}\rvert/\Sigma l_W$
3–4	2	0.019 119 271 7	0.019 516 116 8	0.020
3–5	5	0.023 868 490 5	0.024 391 129 2	0.021
3–6	8	0.024 025 296 7	0.024 547 862 0	0.021
3–7	17	0.025 354 755 3	0.025 884 282 7	0.020
3–8	30	0.025 666 473 8	0.026 197 850 1	0.020
3–9	57	0.026 061 435 5	0.026 593 203 6	0.020
3–10	102	0.026 141 695 2	0.026 673 561 7	0.020
3–11	195	0.026 309 323 4	0.026 841 373 3	0.020
3–12	354	0.026 367 573 2	0.026 899 648 4	0.020
3–13	669	0.026 428 525 3	0.026 960 617 8	0.020
3–14	1236	0.026 460 359 1	0.026 989 552 6	0.020

and the fine-grain sense. The Lebesgue measure of chaos is defined as

$$\mathcal{L}_c=\frac{|\Delta_c|-L_{\mathrm{WB}}^t}{|\Delta_c|}\equiv 1-\mathcal{L}_p, \tag{4.1}$$

where $|\Delta_c|$ is the width of the chaotic region (as the renormal scale) and $\mathcal{L}_p$ is the Lebesgue measure of the periodic windows (window bands) on the parameter axis. Since the scaling of periodic windows results in the scaling law for window bands and these scaling behaviors are related to δ, the chaotic measure $\mathcal{L}_c$ will be the function of the convergent rates δ of the periodic sequences.

B. Approximate analytical formula of chaotic measure $\mathcal{L}_c$ by using merely the convergent rates

To obtain the chaotic measure $\mathcal{L}_c$ from (4.1), we only need to find $|\Delta_c|$ since L_{WB}^t has been given in Sec. III. Because the widths $|\Delta_m|$ $(m=0,1,2,\ldots)$ of the subintervals form the Feigenbaum convergent series, i.e., $|\Delta_{m+1}|\sim|\Delta_m|/\delta(R)$, the width of the chaotic region is

$$|\Delta_c|=\sum_{m=0}^{\infty}|\Delta_m|\approx\frac{|\Delta_0|}{1-\delta^{-1}(R)}. \tag{4.2}$$

Therefore, from (3.10), (4.1), and (4.2), we can use the $L_{\mathrm{WB},0}$ and $|\Delta_0|=\lambda(RL^\infty)-\lambda(R*RL^\infty)$ of the subinterval Δ_0 to give the chaotic measure

$$\mathcal{L}_c\approx 1-\frac{L_{\mathrm{WB},0}}{|\Delta_0|}\equiv\mathcal{L}_{c,0}. \tag{4.3}$$

This shows that the measure $(\mathcal{L}_c)$ normalized to the whole chaotic region Δ_c is the same as that $(\mathcal{L}_{c,0})$ normalized to the subinterval Δ_0. This conclusion can be easily extended as

$$\mathcal{L}_c\approx\mathcal{L}_{c,0}\approx\mathcal{L}_{c,1}\approx\mathcal{L}_{c,2}\approx\cdots\approx\mathcal{L}_{c,m}. \tag{4.4}$$

Substituting (3.6) and (3.8) into (4.3), we can explicitly rewrite (4.3) as

$$\mathcal{L}_c\approx 1-\frac{\Sigma\delta^{-1}(\mathbf{Q})}{[1-\delta^{-1}(R)-\Sigma\delta^{-1}(\mathbf{Q})]|\Delta_0|}. \tag{4.5}$$

This is an approximate analytic formula of the chaotic measure $\mathcal{L}_c$. Here we have used the concise notation Σ for $\Sigma_{\mathbf{Q}\in\wp_\pi}$. Since $|\Delta_0|$ is easy to compute, from (4.5) we can see that computing $\mathcal{L}_c$ depends in fact on computing the sum $\Sigma l_W(\mathbf{Q})\approx\Sigma\delta^{-1}(\mathbf{Q})$ of the window widths of all the MSS primitive words. Table IV lists the numerical data of both $\Sigma\delta^{-1}(\mathbf{Q})$ and $\Sigma l_W(\mathbf{Q})$ for period $p=3$–14. We can see that they have only a minor discrepancy and the contribution of the primitive words of large period is extremely small. For the quadratic map $|\Delta_0|=0.456\,31\cdots$, using $\Sigma_{p=3}^{14}\delta^{-1}(\mathbf{Q})=0.026\,46$, we can obtain $\mathcal{L}_c\approx0.9236$. If we use $\Sigma_{p=3}^{14}l_W(\mathbf{Q})=0.026\,99$ to replace $\Sigma\delta^{-1}(\mathbf{Q})$, then $\mathcal{L}_c\approx0.9221$ (see Table VII). Of these two results, the latter, with the use of $\Sigma l_W(\mathbf{Q})$, is of course more exact.

However, it should be indicated that in the calculation of L_{WB}^t in Sec. III, whatever the sequences of the type $\mathbf{Q}*R*^n$ considered in computing $l_{\mathrm{WB}}(\mathbf{Q})$ or the sequences of the type $R*^m*\mathbf{Q}$ considered in computing $L_{\mathrm{WB},m}$, we have taken the convergent rate $\delta(R)=4.669\,20\cdots$, while this value can only be approached for the large values of n and m. When n or m is small, the convergent rate has some deviation from this value. In particular, for the cases of $n=0,1$ and $m=0,1$, the convergent rates are all smaller than this value. This implies that the real widths of the window bands are larger than the previous calculation, so the above calculation can give only the upper bound of the chaotic measure: $\mathcal{L}_c^u=0.9221$.

C. Chaotic measure $\mathcal{L}_c$ by using theoretical K_f and ideal K_b

As mentioned in Sec. III, (3.4) is not accurate. Using (3.3) instead of (3.4), we can obtain a better result for $\mathcal{L}_c$. This means that we should take

$$B_1=K_f\Sigma l_W(\mathbf{Q})=K_f\Sigma\delta^{-1}(\mathbf{Q}), \tag{4.6}$$

$$L_{\mathrm{WB}}^t=K_b\frac{B_1}{1-B_1} \tag{4.7}$$

TABLE V. Weighted average values of $\delta_n(R)$ and the values of $K_f^i(n)=1+\Sigma_{j=1}^{n}\Pi_{k=1}^{j}\delta_k^{-1}(R)$.

n	$\delta_n(R)$	$K_f^i(n)$
1	2.007 85	1.498 05
2	4.237 71	1.615 57
3	4.552 70	1.641 39
4	4.646 05	1.646 94
5	4.663 99	1.648 14

to replace (3.6) and (3.10). Substituting (4.6) and (4.7) into (4.1), we obtain

$$\mathcal{L}_c \approx 1-\frac{K_b K_f \Sigma\,\delta^{-1}(\mathbf{Q})}{[1-K_f\Sigma\,\delta^{-1}(\mathbf{Q})]|\Delta_c|}. \quad (4.8)$$

Here we do not simply take $|\Delta_c|$ as $K_b|\Delta_0|$ since the ratios $|\Delta_m|/|\Delta_{m+1}|$ of the convergent sequence $\{|\Delta_m|\ (m=0,1,2,\cdots)\}$ have a minor discrepancy from $\delta(R)$.

The parameter value of the PDB accumulation point is $\lambda(R*^{\infty})=1.401\,15\cdots$ and we have $\lambda(RL^{\infty})=2$, which leads to $|\Delta_c|=0.598\,84\cdots$. Therefore, using the theoretical value of K_f and the ideal value of K_b, from (4.8) we can obtain $\mathcal{L}_c=0.9029$. Replacing $\Sigma\delta^{-1}(\mathbf{Q})$ by $\Sigma l_W(\mathbf{Q})$, we can have a more exact value $\mathcal{L}_c=0.9009$.

D. Correction factors and further improved calculation of chaotic measure $\mathcal{L}_c$

To improve further the calculation of $\mathcal{L}_c$, we should investigate the detailed processes of convergence for both the *forward* PDB sequences $\mathbf{Q}*R*^n$ and the *backward* PDB sequences $R*^m*\mathbf{Q}$, respectively.

First, we consider the forward PDB type $\mathbf{Q}*R*^n$, namely, examine the calculation of the window band of $\mathbf{Q}$. Let

$$\delta_n(R)=l_W(\mathbf{Q}*R*^{(n-1)})/l_W(\mathbf{Q}*R*^n). \quad (4.9)$$

Then the width of the window band will be

$$l_{\mathrm{WB}}(\mathbf{Q})=l_W(\mathbf{Q})\left[1+\sum_{n=1}^{\infty}\prod_{k=1}^{n}\delta_k^{-1}(R)\right] \equiv K_f^i l_W(\mathbf{Q})=K_f^i\delta^{-1}(\mathbf{Q}). \quad (4.10)$$

Here the correction factor K_f^i will be improved compared to the theoretical value of K_f in (3.3). In order to give K_f^i, we calculate $\delta_{n,j}(R)$ from (4.9) for all the 30 primitive words $\mathbf{Q}_j$ of period $p=3$–8. Then we take their weighted average value as $\delta_n(R)$, i.e., $\delta_n(R)=\Sigma_j g_{n,j}\delta_{n,j}(R)$, where $g_{n,j}=\delta_{n,j}(R)/\Sigma_i\delta_{n,i}(R)$. Table V lists the values of $\delta_n(R)$ for $n=1$–5. For $n\geqslant 6$, using $\delta_n(R)\approx\delta(R)=4.669\,20\cdots$, one can obtain the limit value of $K_f^i(n)$ as

$$K_f^i \approx 1.648\,46, \quad (4.11)$$

which approaches the theoretical value of K_f in (3.3).

Next we investigate the backward PDB type $R*^m*\mathbf{Q}$, namely, consider the compressing in each subinterval Δ_m. Similarly, let

TABLE VI. Weighted average values of $\tilde{\delta}_m(R)$ and the values of $K_b^i(m)=1+\Sigma_{j=1}^{m}\Pi_{k=1}^{j}\tilde{\delta}_k^{-1}(R)$.

m	$\tilde{\delta}_m(R)$	$K_b^i(m)$
1	3.256 62	1.307 07
2	5.589 47	1.362 00
3	4.628 50	1.373 87
4	4.683 40	1.376 41

$$\tilde{\delta}_m(R)=l_W(R*^{(m-1)}*\mathbf{Q})/l_W(R*^m*\mathbf{Q}). \quad (4.12)$$

Then the total width of all the window bands in the chaotic region will be

$$L_{\mathrm{WB}}^t=L_{\mathrm{WB},0}\left[1+\sum_{m=1}^{\infty}\prod_{k=1}^{m}\tilde{\delta}_k^{-1}(R)\right]\equiv K_b^i L_{\mathrm{WB},0}. \quad (4.13)$$

Similarly, the correction factor K_b^i will be improved comparing with the ideal K_b in (3.10). We still take all the 30 primitive words $\mathbf{Q}_j$ of period $p=3$–8 to calculate $\tilde{\delta}_{m,j}(R)$ from (4.12) and list their weighted average values $\tilde{\delta}_m(R)$ in Table VI ($m=1$–4). For $m\geqslant 5$, using $\tilde{\delta}_m(R)\approx\delta(R)$, we have the limit value of $K_b^i(m)$ as

$$K_b^i \approx 1.377\,10, \quad (4.14)$$

which approaches the ideal K_b in (3.10).

For a further improved calculation of the chaotic measure $\mathcal{L}_c$, after the consideration of (4.10), (4.11), (4.13), and (4.14), we take K_f^i and K_b^i to replace K_f and K_b in (3.6), (3.10), and (4.6)–(4.8). Thus we have

$$\mathcal{L}_c \approx 1-\frac{K_b^i K_f^i \Sigma\,\delta^{-1}(\mathbf{Q})}{[1-K_f^i\Sigma\,\delta^{-1}(\mathbf{Q})]|\Delta_c|}. \quad (4.15)$$

Therefore, from (4.15) we can obtain $\mathcal{L}_c=0.8951$. Replacing $\Sigma\delta^{-1}(\mathbf{Q})$ by $\Sigma l_W(\mathbf{Q})$, we can have a more exact value $\mathcal{L}_c=0.8929$. This coincides with the result by using the Monte Carlo method in Ref. [24].

Table VII shows a comparison of the values of $\mathcal{L}_c$ calculated from (4.5), (4.8), and (4.15). Of these three calculations, (4.15) gives the best result.

V. FRACTAL PROPERTIES OF THE CHAOTIC SET

As we have described in Sec. II D, the structure of each subinterval Δ_m in the chaotic region is completely similar.

TABLE VII. Comparison of the chaotic measure $\mathcal{L}_c$ calculated from formulas (4.5), (4.8), and (4.15). The data in the first line are obtained directly from the formulas. The data in the second line are obtained with replacing $\Sigma\delta^{-1}(\mathbf{Q})$ by $\Sigma l_W(\mathbf{Q})$ in the three formulas, which are better than the first line. Of these three methods, (4.15) gives the best result.

Chaotic measure $\mathcal{L}_c$	(4.5)	(4.8)	(4.15)
using $\Sigma\delta^{-1}(\mathbf{Q})$	0.9236	0.9029	0.8951
using $\Sigma l_W(\mathbf{Q})$	0.9221	0.9009	0.8929

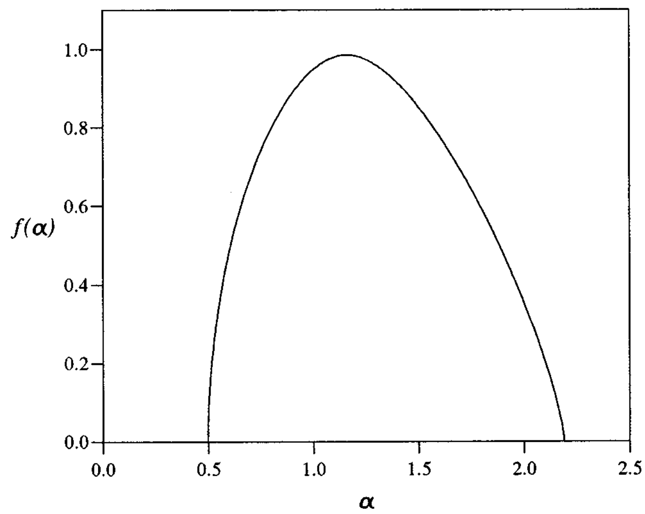

FIG. 2. Curve of the singularity spectrum $f(\alpha)$ for the chaotic set in the subinterval Δ_0.

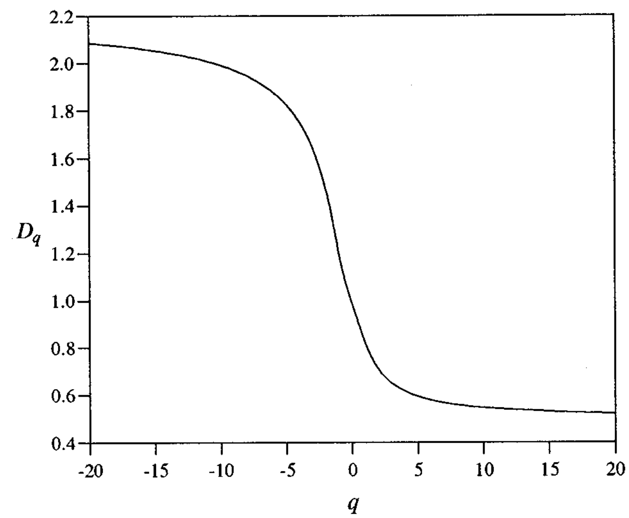

FIG. 3. Curve of the generalized dimension D_q for the chaotic set in the subinterval Δ_0.

Therefore, from the bi-Lipschitz transformation theorem [25,4], one can conclude that the chaotic set in each Δ_m after excluding all the periodic window bands in Δ_m has the same fractal dimension D_0. For this reason, we will concentrate our consideration on only the subinterval Δ_0. After excluding all the infinitely many periodic window bands $l_{\mathrm{WB}}(\mathbf{Q})=K_f^i l_W(\mathbf{Q})$, we can obtain the chaotic set in Δ_0. According to the previous discussion, this is a fractal set of positive measure and infinitely many scales, a point set completely disconnected and nowhere dense in Δ_0 on the parameter axis. Since $\mathcal{L}_c \neq 0$, this chaotic set should theoretically have the Hausdorff dimension $D_H=1$ [25]. It should be indicated that this chaotic set is the *real* chaotic set, while that chaotic set in Ref. [4] is not the real one because in Ref. [4] the contributions of the coarse-grained chaotic sequences contained in each ETEC step have been ignored. Here all the periodic window bands have been excluded, so both the coarse-grained and the fine-grained chaotic sequences are included in the chaotic set.

To save the CPU time we will mainly use the direct method of Chhabra and Jensen [26] rather than the indirect method of Halsey *et al.* [27] to calculate the singularity spectrum $f(\alpha)$ (Fig. 2) and the generalized dimension D_q (Fig. 3). Although it is impossible to exclude infinitely many periodic window bands for the numerical calculation, in fact, one can obtain a very good numerical approach after excluding all the 1236 window bands of the basic period $p=3$–14. Table VIII lists some numerical values of that special sense. We can see that the fractal dimension D_0 is very close to the theoretical result of $D_H=1$ (in general, $D_0=D_H$).

VI. DISCUSSION

From the above we can see the significance of the convergent rates δ. For the quadratic map $f_\lambda(x)=1-\lambda x^2$, not only can the analytic expressions of the periodic windows and the window bands be given by δ but the measure of the chaotic orbits that are completely different from the periodic orbits can also be given explicitly by δ. In particular, we further understand that a series of characteristic scaling constants such as μ_c, γ_{PDB}, and γ_N, even the convergent rate δ itself, originate from the uniform geometric compressibility of the DGP $*$ operation dominated by preserving the equal topological entropy. Moreover, the singularity spectrum and the generalized fractal dimension of the chaotic set are calculated. We thus promoted the understanding to the relation between the chaotic motion and the periodic motion.

It should be noted that in our calculation, the relation (3.1), of crucial importance, is valid for the quadratic map $f_\lambda(x)=1-\lambda x^2$. If the map is replaced by other maps of a quadratic maximum such as the logistic map $f_\mu(x)=\mu x(1-x)$ or $f_\nu(x)=\nu\sin\pi x$, then (3.1) will need some modifications. For example, as the parameter transformation between $f_\mu(x)$ and $f_\lambda(x)$ is $\mu=1+\sqrt{1+4\lambda}$, for the logistic map there will be a function transformation between $l_W(\mathbf{Q})$ and $\delta^{-1}(\mathbf{Q})$, i.e., $l_W(\mathbf{Q})=F(\delta^{-1}(\mathbf{Q}))$. In this case, (3.1) and other relationships in the calculation of the chaotic measure would not be as simple as that for the quadratic map; however, the method of treatment is similar. It is worth noting that for such maps of a quadratic maximum, the ETEC step scaling constant $\mu_c=\frac{9}{4}$ and the window scaling ratios $\gamma_{\mathrm{PDB}}=1$ and $\gamma_N=\frac{1}{3}$ for the superstable positions in the periodic windows are still universal.

Strictly speaking, the universal window scaling ratios γ_{PDB} and γ_N divide all the periodic sequences into two classes: one consists of the PDB cascade sequences $R*^n$ and $\mathbf{A}*R*^n$ $(\mathbf{A}\in\wp)$ to be called $\wp_{\mathrm{PDB}}$ and the other of non-PDB sequences to be called $\wp_N$; each of these two classes has infinitely many sequences. Thus three scaling ratios

$$\frac{|\mathbf{Q}*[L^\infty,RL^\infty]|}{|\mathbf{Q}*[L^\infty,R^\infty]|}\left(\mathbf{Q}\in\bigcup_{m=0}^{\infty}R*^m*\wp_\pi\right),$$

$$\frac{|\mathbf{Q}*[L^\infty,C]|}{|\mathbf{Q}*[C,R^\infty]|}\;(\mathbf{Q}\in\wp_{\mathrm{PDB}}),$$

$$\frac{|\mathbf{Q}*[L^\infty,C]|}{|\mathbf{Q}*[C,R^\infty]|}\;(\mathbf{Q}\in\wp_N)$$

TABLE VIII. Fractal property of the chaotic set in Δ_0.

Method of Chhabra and Jensen [26]	Method of Halsey *et al.* [27]
$f(\alpha(0))=D_0=0.9858$	$D_0=0.9830$
$f(\alpha(1))=\alpha(1)=D_1=0.8180$	$D_1=0.8401$
$\alpha_{\max}=\alpha(-\infty)=D_{-\infty}=2.1910$	
$\alpha_{\min}=\alpha(+\infty)=D_{+\infty}=0.4964$	

form, respectively, three very small intervals [2.17, 2.25], [1, 1.09], and [0.33, 0.36], namely, bound infinite sets of real numbers. According to the classical Bolzano-Weierstrass theorem [28], of course, the scaling ratios μ_c, γ_{PDB}, and γ_N would be limit points of the three infinite sets, respectively. In addition, the last two scaling ratios characterize the global structure of all the periodic windows. This result directly indicates the global regularity of negative Lyapunov exponents. In general, Lyapunov exponents are difficult to deal with analytically for they lack explicit expressions [29]. By γ_{PDB} and γ_N, the global regularity of three important positions $(\lambda_l,\lambda_c,\lambda_r)$ of Lyapunov exponents $(0,-\infty,0)$ in periodic windows is presented; thus the structural pattern of the curve of negative Lyapunov exponents is displayed clearly. It is very useful to construct the global expressions of the curve of characteristic exponent. We believe that the results reveal the global regularities independent of the sequences (words) and make a substantial advancement of metric and scaling universalities; this would be significant for our further construction work on the global thermodynamic formalism of chaotic dynamical systems.

ACKNOWLEDGMENTS

This work was supported in part by the National Basic Research Project (Nonlinear Science) of China, the National Natural Science Foundation of China, and the Applied Basic Research Foundation of Yunnan Province. We thank Xu-Sheng Zhang and Xiao-Dong Liu for their useful discussions.

[1] M. J. Feigenbaum, J. Stat. Phys. **19**, 25 (1978); **21**, 669 (1979).
[2] S.-L. Peng, K.-F. Cao, and Z.-X. Chen, Phys. Lett. A **193**, 437 (1994); **196**, 378 (1995).
[3] Z.-X. Chen, K.-F. Cao, and S.-L. Peng, Phys. Rev. E **51**, 1983 (1995).
[4] K.-F. Cao, Z.-X. Chen, and S.-L. Peng, Phys. Rev. E **51**, 1989 (1995).
[5] B. Derrida, A. Gervois, and Y. Pomeau, Ann. Inst. Henri Poincaré A **29**, 305 (1978).
[6] B. Derrida, A. Gervois, and Y. Pomeau, J. Phys. A **12**, 269 (1979).
[7] H. Kaplan, Phys. Lett. A **97**, 365 (1983).
[8] J. A. Yorke, C. Grebogi, E. Ott, and L. Tedeschini-Lalli, Phys. Rev. Lett. **54**, 1095 (1985).
[9] M. V. Jakobson, Commun. Math. Phys. **81**, 39 (1981).
[10] P. Collet and J.-P. Eckmann, *Iterated Maps on the Interval as Dynamical Systems* (Birkhäuser, Boston, 1980).
[11] N. Metropolis, M. L. Stein, and P. R. Stein, J. Comb. Theory A **15**, 25 (1973).
[12] B.-L. Hao, *Elementary Symbolic Dynamics and Chaos in Dissipative Systems* (World Scientific, Singapore, 1989).
[13] S.-L. Peng and L.-S. Luo, Phys. Lett. A **153**, 345 (1991). The original definition of DGP $*$ composition is as follows: let $\mathbf{Q}=Q_1Q_2\cdots Q_qC\equiv\widetilde{Q}C$ and $\mathbf{S}=S_1S_2\cdots S_sC$, then the compound sequence $\mathbf{Q}*\mathbf{S}=\widetilde{Q}S_1^{t(\mathbf{Q})}\widetilde{Q}S_2^{t(\mathbf{Q})}\widetilde{Q}\cdots\widetilde{Q}S_s^{t(\mathbf{Q})}\widetilde{Q}C$. The details are in Refs. [5, 15].
[14] J. Milnor and W. Thurston, in *Dynamical Systems*, edited by J. C. Alexander, Lecture Notes in Mathematics Vol. 1342 (Springer, Berlin, 1988), p. 465.
[15] S.-J. Chang and J. McCown, Phys. Rev. A **31**, 3791 (1985).
[16] R. Delbourgo and B. G. Kenny, Aust. J. Phys. **38**, 1 (1985).
[17] V. Urumov, J. Phys. A **22**, 2871 (1989).
[18] C. S. Hsu and M. C. Kim, Phys. Rev. A **31**, 3253 (1985).
[19] W.-M. Zheng, J. Phys. A **22**, 3307 (1989).
[20] B.-L. Hao, Physica D **51**, 161 (1991).
[21] K. Shibayama, in *The Theory of Dynamical Systems and its Applications to Nonlinear Problems*, edited by H. Kawakami (World Scientific, Singapore, 1984), p. 124.
[22] G. J. Chaitin, Sci. Am. **232** (5), 47 (1975).
[23] J. Ford, Phys. Today **36** (4), 40 (1983).
[24] Y.-Q. Wang and S.-G. Chen, Acta Phys. Sin. **33**, 341 (1984).
[25] K. Falconer, *Fractal Geometry: Mathematical Foundations and Applications* (Wiley, Chichester, 1990), p. 30. According to the bi-Lipschitz transformation theorem, for any two words $\mathbf{W}_1<\mathbf{W}_2$ with $\mathbf{W}_1$, $\mathbf{W}_2\epsilon\Delta_m$, and $0<C_1\leqslant C_2<\infty$, the following inequality holds: $C_1|[\mathbf{W}_1,\mathbf{W}_2]|\leqslant|[R*\mathbf{W}_1,R*\mathbf{W}_2]|\leqslant C_2|[\mathbf{W}_1,\mathbf{W}_2]|$, where the constants C_1 and C_2 can be chosen around $\delta^{-1}(R)$. One then has $D_0(\Delta_{m+1}^c)=D_0(\Delta_m^c)$; here, Δ_m^c denotes the chaotic set in Δ_m.
[26] A. Chhabra and R. V. Jensen, Phys. Rev. Lett. **62**, 1327 (1989).
[27] T. C. Halsey, M. H. Jensen, L. P. Kadanoff, I. Procaccia, and B. I. Shraiman, Phys. Rev. A **33**, 1141 (1986); **34**, 1601 (1986).
[28] M. Eisenberg, *Topology* (Holt, Rinehart & Winston, New York, 1974), p. 307.
[29] J.-P. Eckmann and D. Ruelle, Rev. Mod. Phys. **57**, 617 (1985).